



OPEN ACCESS

EDITED BY

Mimma Rizzo,
Azienda Ospedaliero Universitaria Consorziale
Policlinico di Bari, Italy

REVIEWED BY

Mengyao Xu,
Huazhong University of Science and
Technology, China
Federica Ciciriello,
University of Bari Aldo Moro, Italy

*CORRESPONDENCE

Shengjie Chen
✉ m18359107370@163.com

†These authors have contributed
equally to this work and share
first authorship

RECEIVED 30 March 2024

ACCEPTED 29 July 2024

PUBLISHED 14 August 2024

CITATION

Liu S, Lv S, Li X, Lu W and Chen S (2024) The
signature genes of cuproptosis associates
with tumor immune microenvironment and
predicts prognosis in kidney renal clear
cell carcinoma.
Front. Oncol. 14:1409620.
doi: 10.3389/fonc.2024.1409620

COPYRIGHT

© 2024 Liu, Lv, Li, Lu and Chen. This is an
open-access article distributed under the terms
of the [Creative Commons Attribution License
\(CC BY\)](https://creativecommons.org/licenses/by/4.0/). The use, distribution or reproduction
in other forums is permitted, provided the
original author(s) and the copyright owner(s)
are credited and that the original publication
in this journal is cited, in accordance with
accepted academic practice. No use,
distribution or reproduction is permitted
which does not comply with these terms.

The signature genes of cuproptosis associates with tumor immune microenvironment and predicts prognosis in kidney renal clear cell carcinoma

Shuhan Liu^{1†}, Shijie Lv^{2†}, Xi Li¹, Weiguo Lu¹ and Shengjie Chen^{1*}

¹Department of Clinical Laboratory, The First Affiliated Hospital of Guangzhou University of Chinese
Medicine, Guangzhou, Guangdong, China, ²Department of Pharmacology, School of Medicine, Jinan
University, Guangzhou, Guangdong, China

Background: Cuproptosis is a new form of cell death, which has great potential to
be developed in tumors treatment. Our study aimed to explore the predictive value
of cuproptosis-related genes (CRGs) in various cancers, with a focus on kidney renal
clear cell carcinoma (KIRC).

Method: A total of 9502 pan-cancer patients from TCGA cohort were enrolled.
The relationships between CRGs and overall survival (OS) or disease-free survival
(DFS) were analyzed. Gene Set Variation Analysis (GSVA) enrichment analysis was
performed to explore the expression differences of CRGs. Multivariate Cox
regression analysis was used to evaluate the association between GSVA scores
and patient survival. KEGG and GO analyses were employed to identify the
biological functions and pathways. The expression and prognostic characteristics
of FDX1 were examined to evaluate the correlation between FDX1 and KIRC. Cell
experiments were conducted to verify whether FDX1 was involved in cuproptosis
of Caki-1 cells induced by Elesclomol.

Results: Positive cuproptosis signature genes(pos.cu.sig) exhibited the
correlation with prognosis in KIRC, and all of these genes showed differential
expression between KIRC and normal tissues. The GSVA score of pos.cu.sig was
associated with excellent survival (HR=0.61, $P<0.05$), which can also serve as an
independent prognostic factor for KIRC. There was a close correlation between
pos.cu.sig and the tumor immune microenvironment in KIRC by KEGG and GO
analysis. FDX1 expression was correlated with KIRC grade and positively
associated with prognosis in KIRC patients. Compared with the control group,
cell proliferation and migration were significantly inhibited, FDX1 expression was
up-regulated, and Fe-S cluster protein content was decreased of Caki-1 cells
after Elesclomol treatment.

Conclusions: This study provides compelling evidence that cuproptosis is closely linked to the prognosis of KIRC. FDX1 holds promise as a viable biomarker and therapeutic target for assessing the effectiveness of tumor immunotherapy in KIRC.

KEYWORDS

cuproptosis, CRGs, tumor immune microenvironment, Fdx1, KIRC

1 Introduction

Copper is an essential trace element involved in various biological processes. Cuproptosis, a copper-dependent form of regulated cell death, is regulated by mitochondrial ferredoxin 1-mediated protein lipoylation which is different from autophagic cell death or traditional apoptosis or necrosis (1). Recent studies showed that the copper levels of both serum and tumor tissues were significantly increased in cancer patients compared to healthy counterparts (2). Maria et al (3) further proved that dysregulation of copper homeostasis may trigger cytotoxicity, alterations in intracellular copper levels may influence the development and progression of cancer.

Cuproptosis regulatory genes are closely related to tumor occurrence and progression (4). Previous studies have reported that cuproptosis plays a vital role in cancer, they screen out a series of cuproptosis-related genes (CRGs) through whole-genome CRISPR-Cas9 selection screen, some CRGs conferred resistance to cuproptosis, such as FDX1, LIPT1, LIAS, DLD, PDHA1, DLAT and PDHB; other CRGs sensitized the cells to cuproptosis, including CDKN2A, GLS and MTF1 (1). However, whether these CRGs are correlated with cancer patient prognosis remains largely unknown. Several genes involved in cuproptosis were identified, which may offer novel strategies to predict the prognosis of cancer patients.

A pan-cancer mRNA expression profile and clinical data were downloaded from The Cancer Genome Atlas (TCGA) database in the present study. CRGs were then used to construct a prognostic multigene signature for cancer patients' survival. Overall, our data indicate that CRGs are correlated with prognosis of KIRC and tumor immune microenvironment, and may be prognostic markers and potential therapeutic targets for KIRC.

2 Materials and methods

2.1 Data collection

A total of 9502 pan-cancer patient samples with publicly available RNA sequencing data were downloaded from the TCGA website (<https://gdc.cancer.gov/>). The gene expression profiles in the TCGA dataset were identified using the “limma” R package.

Data from TCGA are publicly available, so no ethics committee approval was required for this study (5).

2.2 CRGs acquisition

Ten CRGs were acquired from previous research (1).

2.3 Gene set variation analysis

“GSVA” R packages were used to perform GSVA enrichment analysis in heatmaps. The GSVA analysis was conducted using the “c2.cp.kegg.v6.2.symbols” file downloaded from the MSigDB database.

2.4 Gene set enrichment analysis

To investigate the functional enrichment of the prognostic signature, we used GSEA (<http://www.broadinstitute.org/gsea/index.jsp>). We considered pathways related to immune and progression of KIRC to be significantly enriched when a P-value was less than 0.05 and the false discovery rate was less than 0.05 (6).

2.5 Functional enrichment analysis

A Kyoto Encyclopedia of Genes and Genomes (KEGG) and Gene Ontology (GO) analysis based on the DEGs ($|\log_2FC| \geq 1$, FDR < 0.05) between high- and low-score groups was conducted using the “clusterProfiler” R package. With the R package “gsva”, the infiltrating score of 19 immune cells and 22 immune-related functions was calculated using single-sample gene set enrichment analysis (ssGSEA).

2.6 Validation of the prognostic signature

According to the median GSVA score of the pos.cu.sig. gene, KIRC patients were divided into subgroups with low and high

scores. The survival analysis was conducted using Kaplan-Meier survival analysis using the R package *survminer*. The prognostic factors for OS of patients with KIRC were assessed using univariate and multivariate Cox analyses. In addition, a nomogram was developed to further evaluate this prognostic signature's predictive power (6).

2.7 Cell culture

KIRC cells (Caki-1) were obtained from the Cell Bank of Chinese Academy of Sciences (Shanghai, China). Caki-1 cells were cultured in McCoy's 5A medium (Gibco, #12330031) supplemented with 10% fetal bovine serum (Cegrogen, #21014040).

2.8 Cell counting kit-8 assay

Caki-1 cells were seeded into 96-well plates and exposed to Elesclomol (MCE, # HY-12040) for the indicated hours. Then, 10 μ L of CCK-8 (ABKBio, #ABK0011C) was added to the cells, and the cells were cultured at 37°C for 4 hours. Then, the absorbance (OD value) at wavelengths of 450nm was measured with a microplate reader (Thermo, #1410101).

2.9 EdU proliferation assay (imaging and cytometry)

Detection of Elesclomol effect on Caki-1 cells proliferation was performed according to the manual of Hyper Fluor™ 488 azide EdU Imaging Kits (APEXBIO, #K2240) and 6-FAM Azide EdU Flow Cytometry Assay Kits (APEXBIO, #K1176). After treatment by Elesclomol, 10 μ M EdU labeling medium was added to the cell culture to finish co-incubation for two hours. Next, cells were washed with PBS and fixed with 4% paraformaldehyde for 15 min. After washed with PBS and incubated by 0.5% TritonX-100 for 10 min, anti-EdU working solution was added to stain at room temperature for 30 min. Subsequently, the DNA contents were stained with 5 μ g/ml Hoechst 33342 for 30 min. The stained cells were observed under a fluorescent microscope (Leica Microsystems) or resuspended and analyzed on the flow cytometer (BD Bioscience), and data were processed using FlowJo and calculated the average fluorescence intensity.

2.10 Scratch assay

Cells were cultured in a 6 well plate to a confluent monolayer. The cell monolayer was scratched in a straight line with a 200 pipette tip. The culture medium was removed and washed (two times) and replaced with 2 mL culture medium. Images were taken at initial scratch and 24, 48 hours later.

2.11 Quantitative real-time polymerase chain reaction assay

Total RNA was extracted using ABKzol (ABKBio, #ABK0005M). cDNA was synthesized from 1 μ g total RNA using the ABKscript RT MasterMix (OneStep gDNA Removal) (ABKBio, #ABK0004M), and the ABKuniversal SYBR Green qPCR Mix (ABKBio, #ABK0003M) was used for quantitative reverse transcription polymerase chain reaction (qRT-PCR). For analysis, the threshold cycle (Ct) values for each gene were normalized to expression levels of β -Actin. All primers were designed and synthesized by Shangya Biotechnology. The primer sequences used in PCR are as follows: FDX1:5'-CTGGCTTGTTCAACCTGTCA-3'(Forward), 5'CAACCGTGATCTGTCTGTTAGTC-3'(Reverse); β -Actin:5'-TGTCACCTTCCAGCAGATGT-3'(Forward), 5'-AGCTCAGTAACAGTCCGCC TAG-3'(Reverse).

2.12 Western blotting

To evaluate the changes in protein expression by Western blot, cells were lysed with lysis buffer and the protein concentration was determined by a bicinchoninic acid (BCA) protein assay kit (Sigma, #71285-M). Protein lysates (40 μ g) were separated by sodium dodecyl sulfate polyacrylamide gel electrophoresis (SDS-PAGE) and electro-transferred to polyvinylidene difluoride (PVDF) membranes. The membrane was blocked in Trisbuffered saline plus tween-20 containing 5% nonfat powdered milk for 1 h and incubated with primary antibodies such as FDX1 (Affinity, #DF7950) and β -actin (Bioss, #bs-0061R) as well as HRP-conjugated secondary antibodies. HRP luminescence was detected with an enhanced chemiluminescence (ECL) detection kit (Meilunbio, #MA0186). The expression of the target band relative to the loading control was quantified with integrated density by ImageJ software.

2.13 Fe-S cluster content assay

The levels of Fe-S cluster in cells were determined by double antibody sandwich method using Fe-S Cluster Immunoassay Kit (YJBio, #202312). And the experiments were carried out according to the manufacturer's instructions. Cells were homogenized with lysis buffer and the Fe-S cluster in samples reacts with reagent to generate adduct which can be quantified colorimetrically.

2.14 Statistical analysis

This study utilized the Kaplan-Meier method to determine the overall survival (OS) and log-rank tests to identify significant differences. To compare two groups' differences, chi-square, corrected chi-square, and Fisher's exact tests were used for continuous data. Mann-Whitney U was used to compare non-parametric variables. We compared tumor

and nontumor tissue gene expression using the Student's *t*-test. Through univariate Cox regression analyses, we calculated hazard ratios (HRs) for CRGs by using Wald tests, and then identified independent prognostic factors. We then used the forestplot R package to visualize their independent prognostic value, which was then tested by multivariate analysis. The statistical analyses were performed using R (version 3.5.1) or SPSS Statistics 26.0 (IBM, Armonk, NY, USA). All data from experiment are presented as the mean \pm standard error of the mean (SEM). The differences between groups were analyzed using Student's *t*-tests or one-way analysis of variance (ANOVA), and $P < 0.05$ was considered statistically significant.

3 Results

3.1 The prognostic relevance analysis of CRGs in pan-cancer

We extracted 10 CRGs from published articles, including 7 positive cuproptosis signature (pos.cu.sig) genes (FDX1, DLD, LIPT1, LIAS, PDHA1, DLAT and PDHB) and 3 negative cuproptosis signature (neg.cu.sig) genes (CDKN2A, GLS and MTF1) (1). Among 9502 pan-cancer patients from the TCGA cohort, high expression of pos.cu.sig gene was interrelated with higher survival rates, but neg.cu.sig genes were associated with a poor survival rate (Figures 1A, B). Next, we compared OS of pos.cu.sig genes and neg.cu.sig genes in each cancer type, the pos.cu.sig genes of kidney renal clear cell carcinoma (KIRC) were extremely related to prognostic value (Figures 1C, D). Then, we further analyzed the relationships between CRGs and OS or disease-free survival (DFS) in pan-cancer cohorts. Results showed that all pos.cu.sig genes were significantly negatively interrelated the HR of OS and DFS in KIRC, however, the consistent change were not found in neg.cu.sig genes (Figures 1E-H).

3.2 The expression and prognostic characteristics of CRGs in KIRC

To explore the expression differences of CRGs between normal tissue and KIRC, we proceed Gene Set Variation Analysis (GSVA) enrichment analysis. Interestingly, pos.cu.sig genes were downregulated in KIRC tissues contrast with normal adjacent, while there is no difference in neg.cu.sig genes (Figure 2A). At the same time, we showed the expression level of 7 pos.cu.sig genes and 2 neg.cu.sig genes (MTF1 gene expression is lost) in KIRC and normal tissue by box plots. Figure 2B showed that FDX1, DLD, LIPT1, DLAT, PDHA1 and PDHB downregulated in KIRC. While 2 neg.cu.sig genes showed discordant changes in KIRC, with GLS down-regulated and CDKN2A up-regulated (Figure 2C). Univariate Cox regression analysis indicated that Age, Grade, Stage, and TNM stages were prognostic factors for KIRC. Besides, pos.cu.sig GSVA score were significantly associated with excellent survival (HR=0.54, $P < 0.001$) (Figure 2D). In addition, the HR of the pos.cu.sig GSVA score determined by multivariate Cox regression analysis was 0.61 ($P < 0.001$) (Figure 2F), forecasting that the

pos.cu.sig genes were an independent prognostic factor for KIRC. At the meantime, the pos.cu.sig genes had excellent predictive capability for risk of death and 3- and 5- year survival probability (Figures 2E-G).

3.3 Functional analyses in the TCGA cohort

KEGG pathway and GO enrichment analyses were used to determine which biological functions and pathways are associated with pos.cu.sig scores. DEGs of low-score group were obviously enriched in tumor immunosuppressive microenvironment, such as Th1 and Th2 cell differentiation, TNF signaling pathway, Cytokine-cytokine receptor interaction, PD-L1 expression and programmed death-1 (PD-1) checkpoint pathway in cancer, TGF-beta signaling pathway and negative regulation of immune response (Figures 3A, B). Our next step was to use GSEA to elucidate the possible biological mechanisms involved in the progression of KIRC disease. Figures 3C-H showed that TGF-beta signaling pathway, PD-L1 expression and PD-1 checkpoint pathway in cancer, IL-17 signaling pathway, Primary immunodeficiency, Neutrophil extracellular trap formation and Chemokine signaling pathway were activated in the low-score group. Our study further examined the correlation between pos.cu.sig scores and immunity status in KIRC using ssGSEA. Comparing to high-score group, plasma cells, T cells CD8, T cells regulatory (Tregs) in the low-score group were higher ($P < 0.05$, Figure 3I). Consistent with the GO enrichment results, various immunosuppressive molecules in the low-score group, including cytokines and inhibitory receptors, were significantly up-regulated in the KIRC tumor microenvironment ($P < 0.05$, Figure 3J).

3.4 FDX1 expression was correlated with prognosis in KIRC

FDX1 is a key protein in the good control of cuproptosis, to assess the relationship between FDX1 and KIRC prognostic, we investigated FDX1's expression and prognostic features in KIRC. In this study, we compared FDX1 mRNA levels in TCGA_KIRC and GTEX normal kidney tissues and in TCGA_KIRC and TCGA para-cancerous tissues. In KIRC tissues, FDX1 expression was significantly lower than in normal or para-cancerous tissues (Figure 4A). Further, FDX1 expression was significantly correlated with KIRC grade, while low FDX1 expression was related to high pathological grade ($P < 0.001$, Figure 4B). Besides, we found a strong correlation between high FDX1 expression and excellent OS through correlation analysis ($P < 0.001$, Figure 4C). Accordingly, FDX1 expression was positively associated with prognosis in KIRC patients. (Figures 4D-F). What is noteworthy is that the level of FDX1 mRNA increased in KIRC tissue after anti-PD-L1 treatment, indicating that a higher FDX1 level results in a more effective immunotherapy (Figure 4G). Survival analysis in the literature showed that the higher the level of FDX1 mRNA, the better the anti-PD-1 treatment effect in not only KIRC but also melanoma (7) (Figures 4H-J).

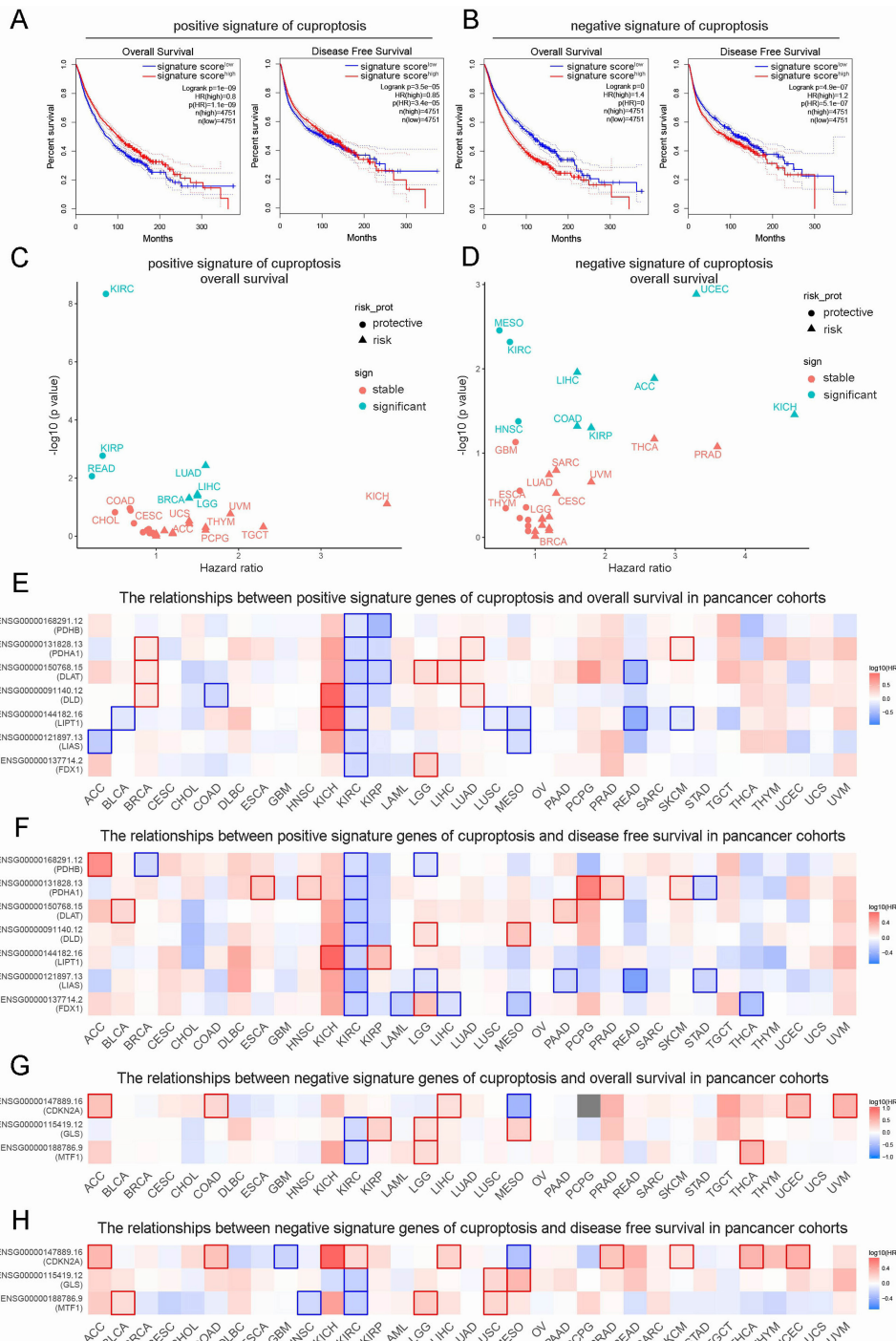
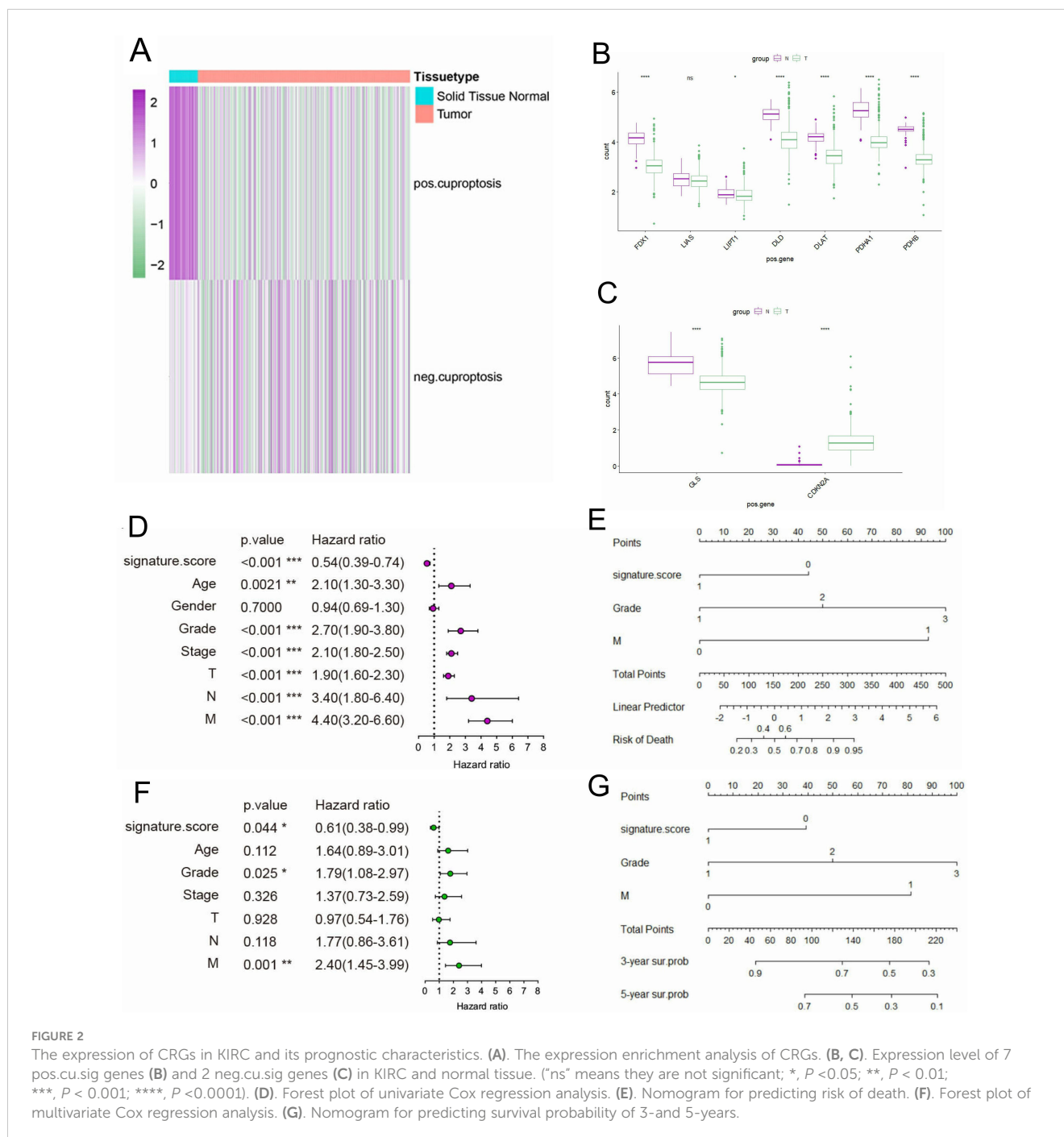


FIGURE 1 Prognostic appraisal of the CRGs signature in pan-cancer. **(A, B)** The correlation of pos.cu.sig genes **(A)** and neg.cu.sig genes **(B)** with OS and DFS in pan-cancer. **(C, D)** The HR and difference significance of pos.cu.sig genes **(C)** and neg.cu.sig genes **(D)** on OS in all TCGA cancer types. **(E, F)** The correlation of each pos.cu.sig genes (n=7) with OS **(E)** and DFS **(F)** in pan-cancer (Borders represent statistically significant differences). **(G, H)** The correlation of each neg.cu.sig genes (n=3) with OS **(G)** and DFS **(H)** in pan-cancer (Borders represent statistically significant differences).

3.5 FDX1 may be involved in cuproptosis of Caki-1 cells induced by Elesclomol

To investigate the effect of Elesclomol on KIRC cells (Caki-1 cells) proliferation and whether FDX1 is involved in regulation. We firstly access the effect of different concentrations Elesclomol (50,

100, 200, 300, 500nM) on Caki-1 cells viability. CCK-8 results showed that the cell viability of Caki-1 cells was decreased after Elesclomol treat for 48h and 72h, and higher concentrations were progressively less viability, but not appear in 24h (Figure 5A). Compared with control group, the EdU staining (Figure 5B) and EdU+ average fluorescence intensity (Figure 5C) of Caki-1 cells

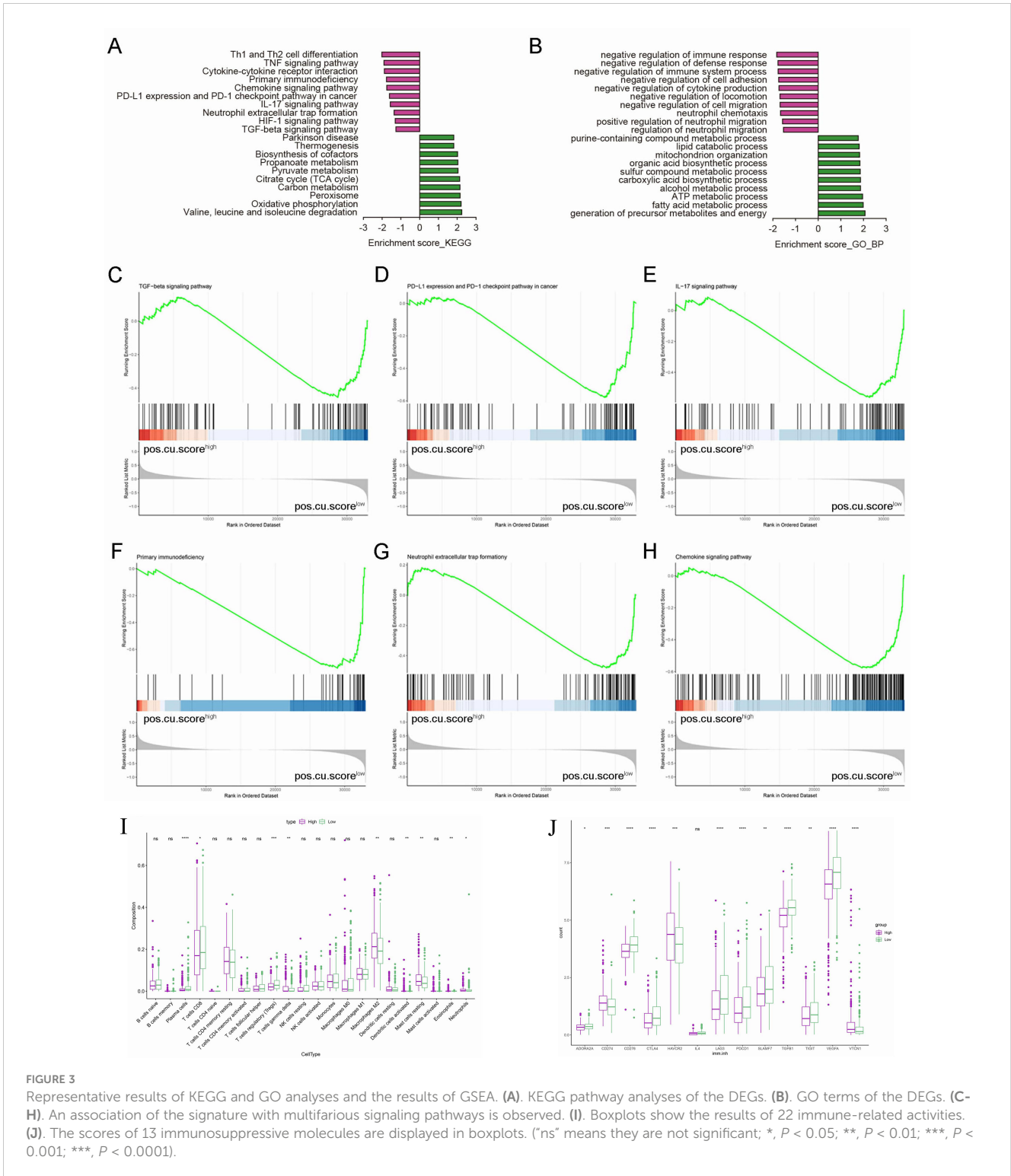


significantly decreased after Elesclomol (500nM) treating for 48h. The scratch assay was used to study the effects of Elesclomol on the migration of Caki-1 cells. The control cells gradually healed after incubating for 24 and 48 hours, while Elesclomol treated cells showed a lower "wound" heal speed after incubation for 24 and 48 hours (Figure 5D). Then qRT-PCR and WB were performed to detect the expression changes of *FDX1* mRNA and protein in Caki-1 cells after Elesclomol (500nM) treating for 48h. The results showed that the *FDX1* gene expression in Caki-1 cells were remarkably elevated after Elesclomol treating (Figures 5E, F, $P < 0.05$). *FDX1* can mediate Fe-S cluster biosynthesis, Fe-S cluster protein reduction is one of the characteristics of cuproptosis (8).

Therefore, we sought to further evaluate the Fe-S cluster protein content of Caki-1 cells after Elesclomol treating. The Fe-S cluster protein content of Elesclomol treated Caki-1 cells decreased significantly compared with the control group (Figure 5G).

4 Discussion

Cuproptosis (1), a new cell death method named in 2022, which is obviously different from the known regulated cell death methods such as apoptosis, necroptosis, pyroptosis and ferroptosis. According to research, cuproptosis is closely associated with



cancer development and prognosis. Our research focused on the correlation between CRGs and of pan-cancer patients based on data extracted from the TCGA database. The OS and DFS of pan-cancer patients was better in pos.cu.sig high-score group, but not in pos.cu.sig low-score group, which indicated that pos.cu.sig maybe a protective factor in tumor patients and plays a tumor suppressor role, while neg.cu.sig generally promotes tumor growth, which was consistent with a recent study that reported that the cuproptosis

level may influence the survival of patients with different tumor types (9).

To determine the correlation of CRGs and the prognosis of specific cancers, we analyzed the association of pos.cu.sig and neg.cu.sig with OS in various cancer types. To our surprise, pos.cu.sig genes can not only be used as a protective factor for KIRC, but also has the most significant prognostic significance in KIRC. In this study, each gene of pos.cu.sig was significantly

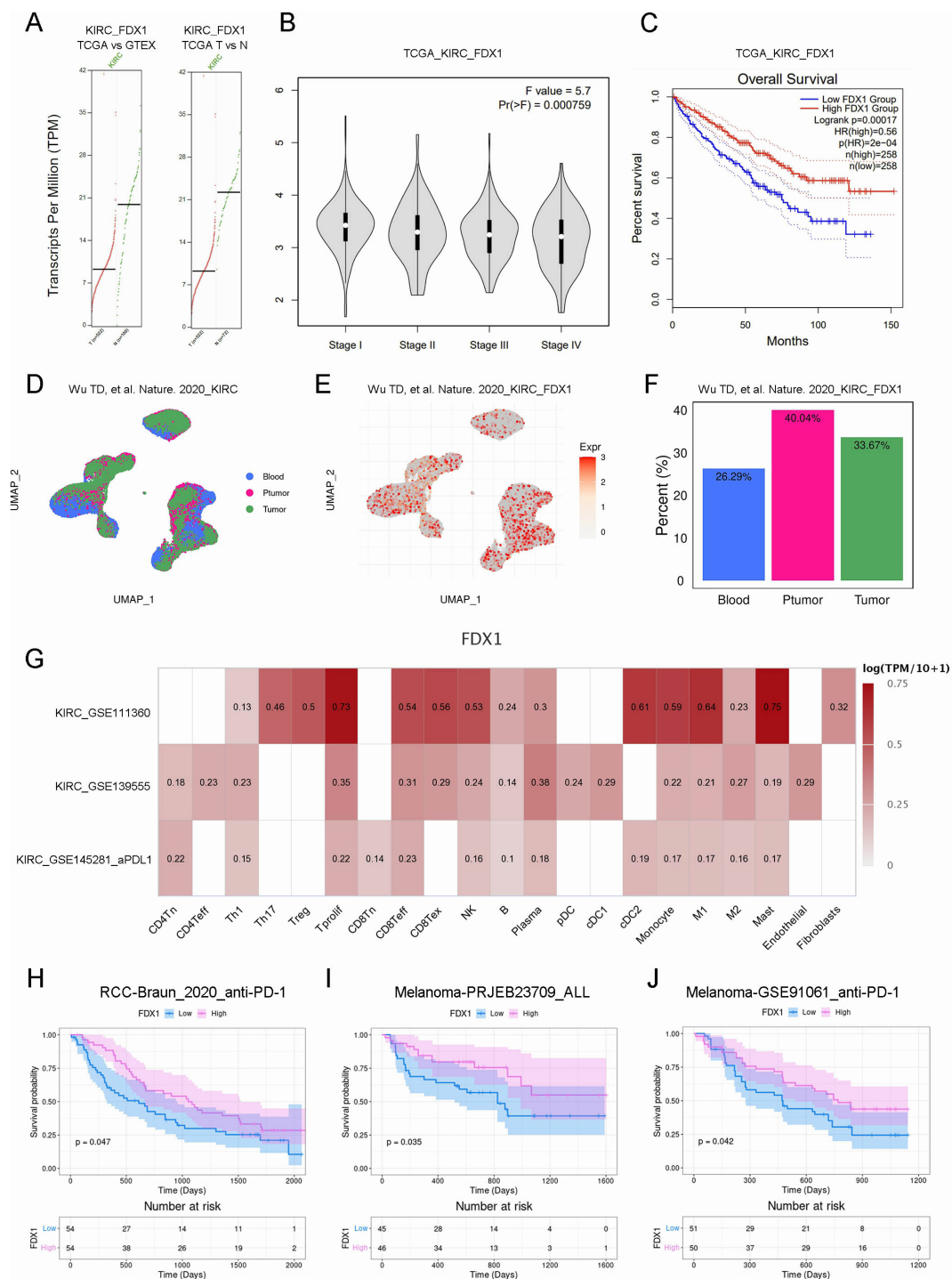


FIGURE 4

FDX1 expression was correlated with prognosis in KIRC patients. (A) The mRNA expression of FDX1 in normal or cancer tissues. (B) The violin plot showed the correlation. (C) The correlation of FDX1 with OS in KIRC. (D-F). The UMAP analyze of FDX1 expression of single-cell sequencing samples. (G). Heat map showed the correlation. (H-J). The Kaplan–Meier survival curve showed the survival probability.

negatively correlated with HR of OS and DFS in KIRC. Besides, all the pos.cu.sig genes were differentially expressed between KIRC and adjacent nontumorous tissues. These results prompted us to focus on the potential role of cuproptosis in KIRC and the possibility of building a prognostic model with these CRGs. Our hypothesis that CRGs may be involved in the regulation of the antitumor process is

supported by the findings of the univariate Cox regression analysis, which showed that pos.cu.sig genes were significantly related to the survival time of KIRC patients. Following that, multivariate Cox regression demonstrated that a new prognostic model incorporating 7 pos.cu.sig genes can separate patients with poor prognosis from those with good prognosis. Compared to the widely

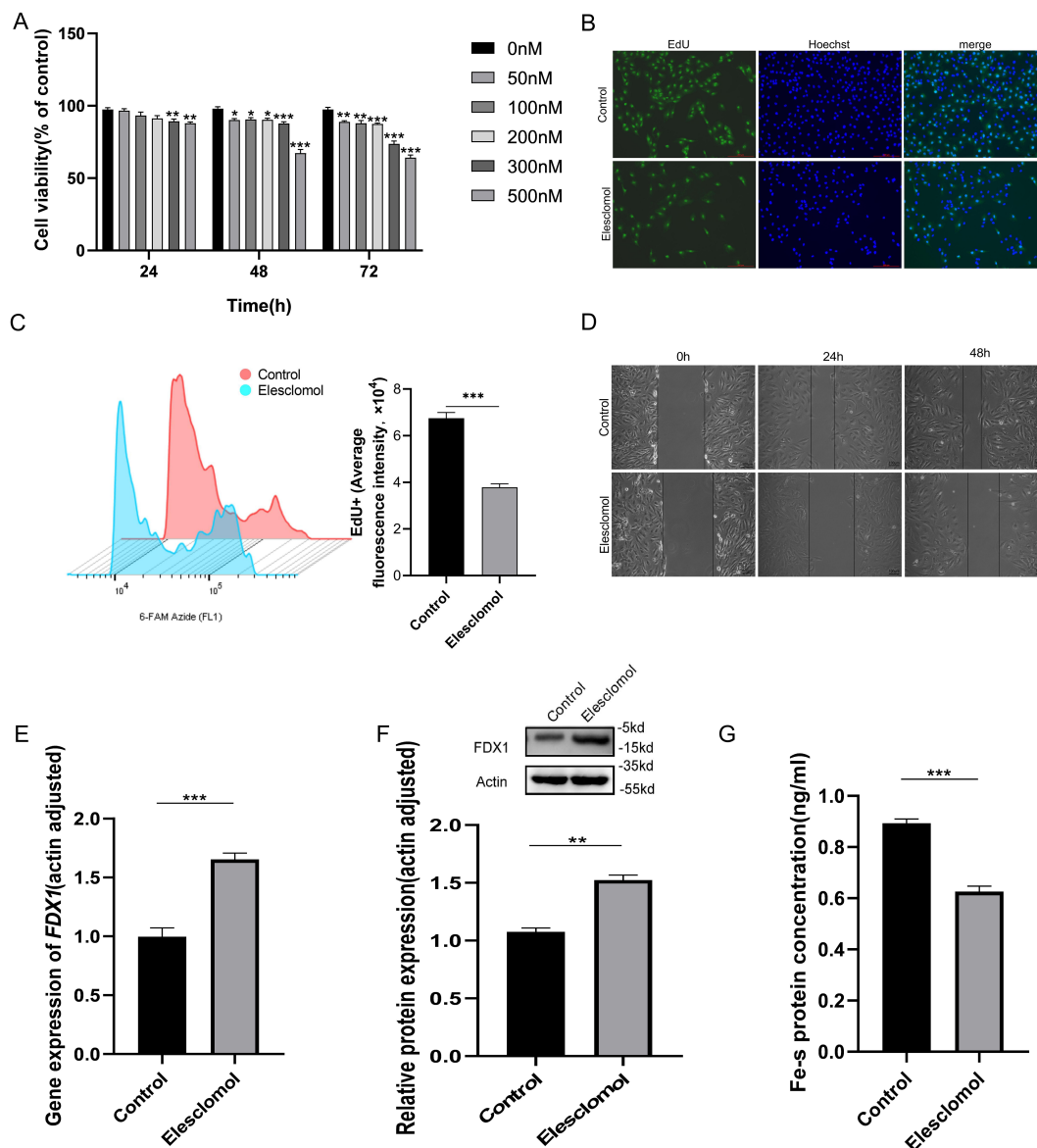


FIGURE 5 Effect of Elesclomol on proliferation and migration of KIRC cells and regulation of FDX1. (A). Caki-1 cells viability was measured using the CCK-8 kit after treating with Elesclomol for 24, 48,72h. (B). EdU staining of Caki-1 cells. Scale bar, 200 μ m; n=3; (C). Caki-1 cell EdU fluorescence intensity analysis by flow cytometry. (D). The healing/closing state of Caki-1cells by the scratch assay (representative pictures from 3 repeated experiments). (E, F). *FDX1* mRNA (E) and protein (F) expression level of Caki-1 cells treated with Elesclomol (500nM) for 48h. (G). The content of Fe-S cluster was tested of Caki-1 cells c treated with Elesclomol (500nM) for 48h. Experiments were repeated three times and the data are expressed as the mean \pm SEM. * $P < 0.05$, ** $P < 0.01$ and *** $P < 0.001$.

used clinical stage, grade, and M stage, this prognostic model performed better for KIRC.

KIRC is one of the most common malignancies, advanced KIRC has an extremely poor prognosis due to its inherent resistance to radiotherapy and chemotherapy (10). KIRC is a highly immune-infiltrating tumor and one of the earliest malignancies to respond to immunotherapy (11). Previous studies have shown that immune cells infiltrating tumor tissue are highly correlated with tumor progression, so they have become the focus of cancer research in recent years (12). Our KEGG and GO analysis results showed that the Th1 and Th2 cell differentiation, TNF signaling pathway,

Cytokine-cytokine receptor interaction, PD-L1 expression and PD-1 checkpoint pathway in cancer, TGF-beta signaling pathway were enriched in the low-score group, which suggest that cuproptosis may be closely related to TIME. Studies have shown that high Th1 cell (13) or low TNF (14) recruiting score is related to the poor prognosis of KIRC patients. Previously, PD-L1 has been reported to act as an accurate biomarker for KIRC, and the agents targeting PD-L1 have had promising effects in renal cell carcinoma (15, 16). In this study, the negative regulation of immune response was obviously activated in the low-score group. One speculation is that cuproptotic cells may regulate the progress of the tricarboxylic

acid cycle (TCA) to affect the activity of immune cells (1, 17). Besides, the increases of T regulatory cells (Tregs), and the decreases of T cells gamma delta ($\gamma\delta$ T cells) and dendritic cells activated represent immunosuppressive status in low-score group patients. It is reported that a large number of Treg cells exist in the tumor microenvironment, Treg cells can inhibit the function of effector T cells and play a key role in tumor immune escape (18). The prognosis of patients with $\gamma\delta$ T cell infiltrating tumor is better than that of patients with other immune cell infiltrating tumors (19). $\gamma\delta$ T can not only kill tumor cells directly, but also activate B/DC/ $\alpha\beta$ T/NK cells indirectly kill tumor cells, so $\gamma\delta$ T cells have become a new research focus in cellular immunotherapy (20). Activated DC cells can trigger the specific immune responses and play an anti-tumor role. Therefore, the weakened antitumor immunity of low-score group patients may lead to KIRC patient poor prognosis. Whether these CRGs play a role in KIRC patients' prognosis by influencing the process of tumor immunity remains to be elucidated, the specific mechanism needs further study.

FDX1 is a ferredoxin in the human mitochondria, studies have confirmed that FDX1 is a key factor for cuproptosis by regulating protein fatty acylation (21). Deletion of FDX1 resulted in the functional loss of protein fatty acylation, the accumulation of pyruvate and α -ketoglutarate and the depletion of succinate in cells, indicating that the functional loss of protein fatty acylation blocks the progression of the TCA (22). Since our previous results have shown that the downregulation of *pos.cu.sig* is closely related to the formation of the tumor immunosuppressive microenvironment in KIRC, we were very curious about the prognostic characteristics of the expression of FDX1 as a cuproptosis core gene in KIRC, and whether it is related to tumor immunotherapy. Consistent with the literature (23), the results showed that FDX1 was underexpressed in KIRC and associated with poor prognosis. More importantly, the immunotherapy data suggested that FDX1 can serve as a potential predictor for the assessment of immunotherapy efficacy in KIRC, with higher FDX1 expression levels leading to better immunotherapy efficacy, which was confirmed in two other melanoma cohorts (7, 24). Then, we conducted cell experiments to verify whether KIRC cells can be induced to cuproptosis by Elesclomol and whether FDX1 is involved in the regulation. Elesclomol is a potent copper ionic carrier that promotes cuproptosis (25). The results of our cell experiments show that Elesclomol can obviously suppressed the cell proliferation and migration of Caki-1 cells. In addition, Elesclomol specifically binds to the $\alpha 2/\alpha 3$ helix and $\beta 5$ chain of FDX1 and inhibits FDX1-mediated Fe-S cluster biosynthesis. Interestingly, the level of mRNA and protein of *FDX1* was up-regulated and Fe-S cluster protein was decreased in Caki-1 cells after Elesclomol treatment. We further inferred that the *FDX1* up-regulation is negatively feedback by the content decrease of Fe-S. In conclusion, the key regulatory gene FDX1 of *pos.cu.sig* genes can be used as a candidate marker and potential therapeutic targets for tumor immunotherapy prognosis evaluation in KIRC.

5 Conclusion

As a result, we developed a new prognostic model using 7 CRGs that has been shown to be independently related to OS and can precisely forecast the prognosis of KIRC. Determining the therapeutic targets for KIRC can be aided by understanding the underlying mechanisms and importance of these CRGs in KIRC. Further research is necessary to better understand the underlying mechanisms relating CRGs to tumor immunity in KIRC.

Data availability statement

All data generated or analyzed during the present study were downloaded from TCGA database (<https://www.cancer.gov/ccg/research/genome-sequencing/tcga>). The RNA-Seq datasets used in this study is based on the UCSC Xena project (<https://xenabrowser.net/datapages/>), which are computed by a standard pipeline.

Ethics statement

Ethical approval was not required for the studies on humans in accordance with the local legislation and institutional requirements because only commercially available established cell lines were used.

Author contributions

SHL: Data curation, Writing – original draft. SJL: Formal analysis, Writing – original draft. XL: Methodology, Writing – review & editing. WL: Conceptualization, Writing – review & editing. SC: Writing – review & editing.

Funding

The author(s) declare that no financial support was received for the research, authorship, and/or publication of this article.

Conflict of interest

The authors declare that the research was conducted in the absence of any commercial or financial relationships that could be construed as a potential conflict of interest.

Publisher's note

All claims expressed in this article are solely those of the authors and do not necessarily represent those of their affiliated organizations, or those of the publisher, the editors and the reviewers. Any product that may be evaluated in this article, or claim that may be made by its manufacturer, is not guaranteed or endorsed by the publisher.

References

- Tsvetkov P, Coy S, Petrova B, Dreishpoon M, Verma A, Abdusamad M, et al. Copper induces cell death by targeting lipoylated TCA cycle proteins. *Science*. (2022) 375:1254–61. doi: 10.1126/science.abf0529
- Ge EJ, Bush AI, Casini A, Cobine PA, Cross JR, DeNicola GM, et al. Connecting copper and cancer: from transition metal signalling to metalloplasia. *Nat Rev Cancer*. (2022) 22:102–13. doi: 10.1038/s41568-021-00417-2
- Babak MV, Ahn D. Modulation of intracellular copper levels as the mechanism of action of anticancer copper complexes: clinical relevance. *Biomedicines*. (2021) 9(8):852. doi: 10.3390/biomedicines9080852
- Siyuan Ma DH, Ping Zhu A. Pan-Cancer Analysis of prognosis and immunity of cuproptosis-related gene FDX1. *PREPRINT*. (2022). doi: 10.21203/rs.3.rs-1632036/v1
- Liang Y, Ye F, Xu C, Zou L, Hu Y, Hu J, et al. A novel survival model based on a Ferroptosis-related gene signature for predicting overall survival in bladder cancer. *BMC Cancer*. (2021) 21:943. doi: 10.1186/s12885-021-08687-7
- Ye Q, Yang X, Zheng S, Mao X, Shao Y, Xuan Z, et al. Low expression of moonlight gene ALAD is correlated with poor prognosis in hepatocellular carcinoma. *Gene*. (2022) 825:146437. doi: 10.1016/j.gene.2022.146437
- Braun MW, Abdelhakim H, Li M, Hyter S, Pessetto Z, Koestler DC, et al. Adherent cell depletion promotes the expansion of renal cell carcinoma infiltrating T cells with optimal characteristics for adoptive transfer. *J Immunother Cancer*. (2020) 8(2):e000706. doi: 10.1136/jitc-2020-000706
- Huo S, Wang Q, Shi W, Peng L, Jiang Y, Zhu M, et al. ATF3/SPI1/SLC31A1 signaling promotes cuproptosis induced by advanced glycosylation end products in diabetic myocardial injury. *Int J Mol Sci*. (2023) 24(2):1667. doi: 10.3390/ijms24021667
- Changwu W, Xiangyu W, Chaoying Q, Wenyong L, Yimin P, Yuzhe L, et al. Pan-cancer analyses reveal molecular and clinical characteristics of cuproptosis regulators in cancer. *PREPRINT*. (2022). doi: 10.21203/rs.3.rs-1652748/v1
- Makhov P, Joshi S, Ghatalia P, Kutikov A, Uzzo RG, Kolenko VM. Resistance to systemic therapies in clear cell renal cell carcinoma: mechanisms and management strategies. *Mol Cancer Ther*. (2018) 17:1355–64. doi: 10.1158/1535-7163.MCT-17-1299
- Wang B, Chen D, Hua H. TBC1D3 family is a prognostic biomarker and correlates with immune infiltration in kidney renal clear cell carcinoma. *Mol Ther Oncolytics*. (2021) 22:528–38. doi: 10.1016/j.omto.2021.06.014
- Oliver AJ, Lau PKH, Unsworth AS, Loi S, Darcy PK, Kershaw MH, et al. Tissue-dependent tumor microenvironments and their impact on immunotherapy responses. *Front Immunol*. (2018) 9:70. doi: 10.3389/fimmu.2018.00070
- Shi B, Qi J. The prognostic value and potential subtypes of immune activity scores in three major urological cancers. *J Cell Physiol*. (2021) 236:2620–30. doi: 10.1002/jcp.30018
- Zhang W, Li C, Wu F, Li N, Wang Y, Hu Y, et al. Analyzing and validating the prognostic value of a TNF-related signature in kidney renal clear cell carcinoma. *Front Mol Biosci*. (2021) 8:689037. doi: 10.3389/fmolb.2021.689037
- Liao KL, Watt KD. Mathematical modeling for the combination treatment of IFN- γ and anti-PD-1 in cancer immunotherapy. *Math Biosci*. (2022) 353:108911. doi: 10.1016/j.mbs.2022.108911
- Massari F, Santoni M, Ciccarese C, Santini D, Alfieri S, Martignoni G, et al. PD-1 blockade therapy in renal cell carcinoma: current studies and future promises. *Cancer Treat Rev*. (2015) 41:114–21. doi: 10.1016/j.ctrv.2014.12.013
- Elia I, Rowe JH, Johnson S, Joshi S, Notarangelo G, Kurmi K, et al. Tumor cells dictate anti-tumor immune responses by altering pyruvate utilization and succinate signaling in CD8(+) T cells. *Cell Metab*. (2022) 34:1137–1150.e6. doi: 10.1016/j.cmet.2022.06.008
- Watson MJ, Vignali PDA, Mullett SJ, Overacre-Delgoffe AE, Peralta RM, Grebinoski S, et al. Metabolic support of tumor-infiltrating regulatory T cells by lactic acid. *Nature*. (2021) 591:645–51. doi: 10.1038/s41586-020-03045-2
- Ren H, Li W, Liu X, Zhao N. $\gamma\delta$ T cells: The potential role in liver disease and implications for cancer immunotherapy. *J Leukoc Biol*. (2022) 112:1663–8. doi: 10.1002/JLB.5MR0822-733RRR
- Silva-Santos B, Mensurado S, Coffelt SB. $\gamma\delta$ T cells: pleiotropic immune effectors with therapeutic potential in cancer. *Nat Rev Cancer*. (2019) 19:392–404. doi: 10.1038/s41568-019-0153-5
- Xiao C, Yang L, Jin L, Lin W, Zhang F, Huang S, et al. Prognostic and immunological role of cuproptosis-related protein FDX1 in pan-cancer. *Front Genet*. (2022) 13:962028. doi: 10.3389/fgene.2022.962028
- Tsvetkov P, Detappe A, Cai K, Keys HR, Brune Z, Ying W, et al. Mitochondrial metabolism promotes adaptation to proteotoxic stress. *Nat Chem Biol*. (2019) 15:681–9. doi: 10.1038/s41589-019-0291-9
- Zhang C, Zeng Y, Guo X, Shen H, Zhang J, Wang K, et al. Pan-cancer analyses confirmed the cuproptosis-related gene FDX1 as an immunotherapy predictor and prognostic biomarker. *Front Genet*. (2022) 13:923737. doi: 10.3389/fgene.2022.923737
- Wu TD, Madireddi S, de Almeida PE, Banchereau R, Chen YJ, Chitre AS, et al. Peripheral T cell expansion predicts tumor infiltration and clinical response. *Nature*. (2020) 579:274–8. doi: 10.1038/s41586-020-2056-8
- Guo B, Yang F, Zhang L, Zhao Q, Wang W, Yin L, et al. Cuproptosis induced by ROS responsive nanoparticles with elesclomol and copper combined with α PD-L1 for enhanced cancer immunotherapy. *Adv Mater*. (2023) 35:e2212267. doi: 10.1002/adma.202212267